Stem Cell Research 16 (2016) 651–661

Contents lists available at ScienceDirect

Stem Cell Research

journal homepage: www.elsevier.com/locate/scr

The Forkhead box transcription factor FOXM1 is required for the maintenance of cell proliferation and protection against oxidative stress in human embryonic stem cells

C.T.D. Kwok [a], M.H. Leung [a], J. Qin [a,d], Y. Qin [a], J. Wang [c], Y.L. Lee [b,*], K.-M. Yao [a,*]

[a] School of Biomedical Sciences, LKS Faculty of Medicine, The University of Hong Kong, Hong Kong, China
[b] Department of Obstetrics and Gynaecology, LKS Faculty of Medicine, The University of Hong Kong, Hong Kong, China
[c] Centre for Genomic Sciences, LKS Faculty of Medicine, The University of Hong Kong, Hong Kong, China
[d] School of Life Sciences, The Chinese University of Hong Kong, Hong Kong, China

ARTICLE INFO

Article history:
Received 9 October 2015
Received in revised form 5 March 2016
Accepted 17 March 2016
Available online 24 March 2016

Keywords:
FOXM1
Human embryonic stem cells
Cell proliferation
Oxidative stress
Chromatin immunoprecipitation-sequencing
Pluripotency

ABSTRACT

Human embryonic stem cells (hESCs) exhibit unique cell cycle structure, self-renewal and pluripotency. The Forkhead box transcription factor M1 (FOXM1) is critically required for the maintenance of pluripotency in mouse embryonic stem cells and mouse embryonal carcinoma cells, but its role in hESCs remains unclear. Here, we show that FOXM1 expression was enriched in undifferentiated hESCs and was regulated in a cell cycle-dependent manner with peak levels detected at the G2/M phase. Expression of *FOXM1* did not correlate with *OCT4* and *NANOG* during in vitro differentiation of hESCs. Importantly, knockdown of FOXM1 expression led to aberrant cell cycle distribution with impairment in mitotic progression but showed no profound effect on the undifferentiated state. Interestingly, FOXM1 depletion sensitized hESCs to oxidative stress. Moreover, genome-wide analysis of FOXM1 targets by ChIP-seq identified genes important for M phase including *CCNB1* and *CDK1*, which were subsequently confirmed by ChIP and RNA interference analyses. Further peak set comparison against a differentiating hESC line and a cancer cell line revealed a substantial difference in the genomic binding profile of FOXM1 in hESCs. Taken together, our findings provide the first evidence to support FOXM1 as an important regulator of cell cycle progression and defense against oxidative stress in hESCs.

1. Introduction

Human embryonic stem cells (hESCs) are undifferentiated cells derived from the inner cell mass of human blastocysts in the pre-implantation stage (Thomson et al., 1998; Trounson, 2006; Pera and Tam, 2010). The hESCs are characterized by the capacity to generate any cell type of all three germ layers (pluripotency) and to grow indefinitely in an undifferentiated state (self-renewal) (Pera and Tam, 2010; Young, 2011). They also have a uniquely short cell cycle with an abbreviated G1 phase (Becker et al., 2006). Thanks to these remarkable properties, hESCs hold great promise for the development of tissue replacement therapy and provide a model system for the study of early embryonic development and lineage specification (Trounson, 2006).

The molecular control of pluripotency and self-renewal in hESCs is attributed to an interactive network of transcription factors. OCT4, NANOG and SOX2 are uniquely expressed in pluripotent cells to orchestrate the transcriptional regulation of pluripotency by collaboratively activating the transcription of one another, constituting an autoregulatory circuitry (Boyer et al., 2005; Young, 2011). These three factors are responsible for driving the expression of genes essential to pluripotency and self-renewal (Boyer et al., 2005; Young, 2011). Regulation of this complex transcriptional network in stem cells deserves further analysis to fully understand the molecular basis of the initiation and maintenance of pluripotency/self-renewal and its pliability.

FOX transcription factors display a vast diversity of biological functions, including cell proliferation, metabolism, apoptosis and differentiation (Myatt and Lam, 2007). Recent studies revealed the involvement of FOX factors in the regulation of self-renewal and pluripotency in embryonic stem (ES) cells. In particular, downregulation of FOXD3 in hESCs was shown to disrupt self-renewal and lead to cell

Abbreviations: hESCs, human embryonic stem cells; ES cells, embryonic stem cells; CDK, cyclin-dependent kinases; EC cells, embryonal carcinoma cells; EB, embryoid bodies; PI, propidium iodide; ROS, reactive oxygen species; GO, gene ontology; RPE, retinal pigment epithelium; RA, retinoic acid; bFGF, basic fibroblast growth factor 2; CM, conditioned medium; DE, definitive endoderm; AVBF medium, medium based on Stemline II Hematopoietic Stem Cell expansion medium supplemented with BMP4; hFF, human foreskin fibroblast; PH3, phosphorylation of histone H3 at Ser10.

* Corresponding authors.
E-mail addresses: cherielee@hku.hk (Y.L. Lee), kmyao@hku.hk (K.-M. Yao).

http://dx.doi.org/10.1016/j.scr.2016.03.007

differentiation towards the endoderm and mesoderm lineages (Arduini and Brivanlou, 2012), whereas FOXO1 was found to be essential for the regulation of hESC pluripotency via the direct transcriptional activation of *OCT4* and *SOX2* (Zhang et al., 2011).

The proliferation-associated FOX factor FOXM1 plays important roles in the regulation of cell proliferation, metastasis, apoptosis and DNA damage repair (Wierstra, 2013b). Studies using various cell models have shown that FOXM1 is essential for proper cell cycle progression by regulating the G1/S and G2/M transitions and the execution of the mitotic program (Laoukili et al., 2005; Wang et al., 2005; Wonsey and Follettie, 2005; Laoukili et al., 2007). FOXM1 activates the expression of the cell cycle genes *CCNB1*, *CCNB2*, *CDC25B* and *PLK1*, which in turn leads to the activation of cyclin-dependent kinases (CDKs), thereby propelling cells through different cell cycle phases (Leung et al., 2001; Wang et al., 2002, 2005; Wonsey and Follettie, 2005).

Recent reports have indicated the functional significance of FOXM1 in pluripotent cells. FOXM1 is required for the maintenance of pluripotency in mouse embryonal carcinoma (EC) cells, via direct regulation of *Oct4* transcription (Xie et al., 2010). More importantly, FOXM1 is important for maintaining pluripotency in mouse ES cells as a downstream target of the LIF/STAT3 signaling pathway, thereby stimulating the expression of pluripotent genes (Tan et al., 2014). Depleting FOXM1 in mouse ES cells led to a rapid loss of pluripotency as well as a decreased rate of cell proliferation (Tan et al., 2014). A recent study in human EC cells provided evidence that FOXM1 is required for *OCT4* expression, underscoring the potential functional role of FOXM1 in the context of human pluripotent stem cells (Chen et al., 2015). However, a detailed study of the expression and function of FOXM1 in hESCs is still lacking.

In this study, we investigated the role of FOXM1 in the regulation of pluripotency and cell proliferation in hESCs. We demonstrated that FOXM1 was expressed in undifferentiated hESCs in a cell cycle-dependent manner, with peak levels reached at the G2/M phase. We showed that FOXM1 depletion had subtle effects on the undifferentiated state of hESCs, but led to the downregulation of cell cycle genes and a delay in G2/M phase progression. Survival of hESCs under oxidative stress was also compromised when FOXM1 was depleted. Interestingly, genome-wide analysis of FOXM1 binding genomic sequences revealed FOXM1 targets and putative cooperative factors, which differ significantly from data previously reported in cancer cells. Our results highlight the important roles played by FOXM1 in maintaining the proliferation and survival of hESCs.

2. Materials and methods

2.1. Cell culture and differentiation

The human embryonic stem cell line VAL-3, obtained from the Spanish Stem Cell Bank (Valbuena et al., 2006), was cultured on plates coated with BD Matrigel™ hESC-qualified Matrix (BD Biosciences, USA) in mTeSR™1 Maintenance Medium (STEMCELL Technologies, Canada) at 37 °C in 5% CO_2 (Ludwig et al., 2006). Cell passage was performed by enzymatic dissociation using Accutase (Invitrogen), and culture media were supplemented with 10 μM ROCK inhibitor (Y-27632; Millipore) for the first day after cell seeding. Spontaneous differentiation was initiated by the formation of embryoid bodies (EB) from VAL-3 cells as previous described (Chen et al., 2012). Details of EB formation and other in vitro differentiation protocols are described in the Supplementary material (Extended methods).

2.2. FOXM1 knockdown

FOXM1 was depleted by RNA interference (RNAi) using short interfering RNA (siRNA). Cy3-labeled siRNA duplexes, of which two were against FOXM1 (FOXM1 siRNA #1: 5′-CUC UUC UCC CUC AGA UAU A-3′; FOXM1 siRNA #2: 5′-GGA AAU GCU UGU GAU UCA ACA-3′) and one was a non-specific siRNA control (Silencer® Cy3-labeled Negative Control No.1 siRNA), were purchased from Ambion® (Life Technologies) as in previous studies (Kong et al., 2013; Liu et al., 2013). Transfection of cells with siRNAs (25 nM) was performed with Lipofectamine RNAiMAX (Life Technologies) according to the manufacturer's protocol.

2.3. Quantitative real-time PCR and immunoblot analyses

Real-Time quantitative PCR (qPCR) and immunoblot analyses were performed with the use of *mir*Vana™ PARIS™ Kit (Ambion®; Life Technologies) as previously described (Chen et al., 2012). FAM-labeled primers for genes of interest are listed in Supplementary Table 1. For details of antibodies and procedures, please see the Supplementary material (Extended methods).

2.4. Immunofluorescence

Cells were fixed with 4% paraformaldehyde (PFA), permeated with 0.1% Triton X-100 in PBST and then blocked with 3% BSA in PBST. After treatment with mouse anti-FOXM1 (ab55006; 1:100; Abcam), rabbit anti-OCT4 (H-134; 1:100; Santa Cruz), rabbit anti-phospho-histone H3 Ser 10 (PH3) (06–570; 1:500; Upstate) or mouse anti-SSEA-1 (MAB4301; 1:128; Millipore), cells were incubated with goat anti-rabbit IgG Alexa Fluor ® 488, goat anti-rabbit IgG Alexa Fluor ® 568, goat anti-mouse IgG Alexa Fluor ® 488 or goat anti-mouse IgG Alexa Fluor ® 568 (Invitrogen). Nuclear counterstaining was performed by incubation with 1:1000 Hoechst 33258 (Invitrogen), and images were taken using the confocal microscope LSM 700 (Carl Zeiss). For PH3 staining, the number of cells positive for PH3 was counted in at least four randomly selected fields at 100× magnification, comprising at least 1000 cells. Cells at different mitotic phases (prophase, prometaphase, or metaphase/anaphase/telophase) were judged based on the chromosome staining pattern as previously described (Neganova et al., 2014).

2.5. Flow cytometric analysis

Cell pellets containing 1×10^6 cells were collected and fixed with ice-cold 100% methanol. For cell cycle profiling, fixed cells were resuspended in Flow Staining Buffer containing 1:8333 Hoechst 33258 for DNA staining prior to flow cytometric analysis. Raw data obtained were analyzed with Modfit TM LT version 4.0 (Verity software). For bivariate flow cytometric analysis, fixed cells were blocked in 1% BSA, and then incubated with 1 μg mouse anti-FOXM1 (Abcam) (in 100 μl). Isotypic control was prepared by incubating cells with normal mouse IgG (Millipore) rather than FOXM1 antibody. Cells were then incubated with goat anti-mouse IgG Alexa Fluor ® 488 (Invitrogen) and resuspended in propidium iodide (PI) solution (0.5 mg/ml PI, 0.1 g RNase A, 0.5 g/ml Triton X-100). Cells were subjected to flow cytometric analysis in a BD LSR Fortessa Analyzer (BD Biosciences). Data were acquired by BD FACSDiva Software (BD Biosciences) and analyzed with FlowJo version 8.0 (FlowJo, LLC).

2.6. Cell proliferation assay

Cell growth after FOXM1 knockdown and/or hydrogen peroxide treatment were quantified by cell counting using the CyQUANT® NF Cell Proliferation Assay Kit (Life Technologies) according to the manufacturer's instruction. Details of the assay are given in Supplementary material (Extended methods).

2.7. ROS assay

To detect the cellular level of reactive oxygen species (ROS), assay using chloromethyl derivative of 2′,7′-dichlorodihydrofluorescein

diacetate (CM-H_2DCFDA; Invitrogen) was performed according to manufacturer's instruction. For details, please see Supplementary material (Extended methods).

2.8. ChIP, ChIP-seq and ChIP–qPCR assays

Chromatin immunoprecipitation (ChIP) assays were performed as previously described (Bramswig et al., 2013), using FOXM1 antibody (C20; Santa Cruz) and control IgG (Millipore). Briefly, VAL-3 cells were treated with 1% paraformaldehyde for chromatin cross-linking before cell lysis and sonication to generate DNA fragments. Fragmented chromatin mixed with Dynabeads protein G (Life Technologies) was incubated with either FOXM1 antibody or rabbit IgG at 4 °C overnight. Successive rounds of magnetic clearance were performed, followed by crosslink reversal with NaCl incubation and protein digestion with proteinase K. DNA was purified using the Wizard® PCR clean-up system (Promega). For ChIP-seq, ChIPed DNA and input DNA were amplified before library construction, and sequencing was carried out using an Illumina HiSeq 2000 genome analyzer (by BGI, China). Enrichment of FOXM1 at specific promoters was verified by quantitative PCR using specific primers of sequences obtained by personal communication with Chen et al. (2013). Quantitative PCR was carried out in duplicate for at least three biological replicates, using SYBR® Select Master Mix (Life Technologies).

2.9. Computational analysis

Sequence reads obtained from FOXM1 ChIP-seq were aligned against the hg19 genome (UCSC Genome Browser) using Bowtie2 (Langmead et al., 2009), and peaks were called using MACS (version 2.1.0) (Zhang et al., 2008). Gene annotation was performed by assigning peaks to the nearest genes using HOMER (Heinz et al., 2010). Motif discovery was performed using MEME and DREME (Bailey and Elkan, 1994; Bailey, 2011), and the motifs were matched with known DNA binding motifs using TOMTOM (Gupta et al., 2007). Gene Ontology (GO) analyses were performed using DAVID (Huang et al., 2009a; Huang et al., 2009b).

Peaks of both the OE33 and retinal pigment epithelium (RPE) datasets (deposited to ArrayExpress under accession number E-MTAB-4121 and E-MTAB-3137, respectively) were recalled using the same reference genome (hg19) and same versions of bioinformatics tools. Our VAL-3 dataset (deposited to the GEO repository at NCBI under accession number GSE79694) validated by ChIP–qPCR corresponds to a high coverage dataset. To generate high coverage datasets for both OE33 and RPE, ChIP and control samples were separately pooled as inputs to MACS2 for peak calling. This analysis generates 1268 peaks and 1221 peaks for OE33 and RPE, respectively, which are comparable in number to our VAL-3 dataset with 1377 peaks to ensure fair comparison. Peak comparison was performed with the use of Bedtools (Quinlan and Hall, 2010). Details of statistical analysis are given in Supplementary material (Extended methods).

3. Results

3.1. FOXM1 is expressed in a cell cycle phase-dependent manner in undifferentiated hESCs

To unveil its potential role during early human development, we examined FOXM1 expression in undifferentiated hESCs. FOXM1 expression diminishes in terminally differentiated cells but is markedly upregulated in various cancer cell lines (Laoukili et al., 2007). Both immunoblot and qPCR analyses showed that FOXM1 expression was enriched in the hESC line VAL-3 (pluripotency reflected by *OCT4* and *NANOG* expression) when compared to human foreskin fibroblasts (hFFs), which are terminally differentiated (Fig. 1 A and B). FOXM1 expression in hESCs was lower than in HeLa cells (Fig. 1 A and B). Immunofluorescence analysis revealed a predominant nuclear localization of FOXM1 in VAL-3 (Fig. 1C) as in mouse ES cells (Tan et al., 2014). FOXM1 co-localized with the pluripotent marker OCT4 in VAL-3 (Fig. 1C). To examine whether FOXM1 expression in VAL-3 is cell cycle phase-dependent, we performed bivariate flow cytometric analysis to correlate FOXM1 levels with DNA content (Fig. 1D). Cells expressed FOXM1 at all cell cycle phases, but there was an obvious upsurge of FOXM1 when cells entered the G2 and M phases of the cell cycle. Signal quantification indicated 67.0% ($P < 0.05$) upregulation of FOXM1 expression at G2/M compared to G1 phase and 49.1% ($P < 0.05$) upregulation compared to S phase (Fig. 1E).

3.2. FOXM1 expression in differentiated hESCs

To test whether FOXM1 plays a role in the regulation of stem cell pluripotency, we examined the temporal expression of *FOXM1* and the core pluripotent marker genes *OCT4* and *NANOG* by qPCR during the spontaneous differentiation of VAL-3 cells at four-day intervals until 24 days of embryoid body (EB) formation. As shown in Fig. 2A, EB differentiation of hESCs led to a dramatic reduction of *OCT4* and *NANOG* transcripts ($P < 0.01$), but there was substantial discrepancy in *FOXM1* mRNA levels among the VAL-3 EB samples collected. FOXM1 levels appeared to fluctuate at all stages of EB differentiation, as indicated by the large error bars (Fig. 2A).

Retinoic acid (RA) is a potent inducer, driving hESC differentiation towards a number of specific lineages in vitro (Gudas and Wagner, 2011; Jagtap et al., 2013). Given that RA-induced differentiation led to rapid depletion of FOXM1 in mouse EC cells (Xie et al., 2010), it would be interesting to know whether RA induces a similar effect on hESCs. VAL-3 cells were induced to differentiate with 5 μM RA, whereas control cells were treated with basic fibroblast growth factor 2 (bFGF). VAL-3 colonies subjected to RA treatment underwent dramatic morphological change indicative of rapid differentiation; increasingly compact cell clusters emerged from monolayers of adherent cells (Supplementary Fig. 1). Expression of core pluripotent marker genes diminished promptly after the initiation of differentiation (Fig. 2B and C). In contrast, *FOXM1* expression remained high until day 5 and declined starting from day 7 ($P < 0.05$) (Fig. 2D). The efficiency of hESC differentiation initiated by RA was confirmed by elevated levels of differentiation marker genes in RA-induced hESCs, including *PAX6* (ectodermal) and *GATA6* (primitive endodermal) (Supplementary Fig. 2).

To gain further insight into *FOXM1* expression during differentiation towards other early lineages, we subjected VAL-3 cells to other differentiation protocols. VAL-3 cells were induced to differentiate towards the trophectodermal lineage by incubation with BMP4 for nine days (Golos et al., 2006). We observed significant downregulation of *FOXM1* transcripts accompanied by the depletion of *OCT4* and *NANOG* mRNAs (Fig. 2E). However, when VAL-3 cells were induced to endoderm derivatives using the STEMdiff™ Definitive Endoderm kit, no significant reduction in *FOXM1* level was observed after five days of differentiation, while *OCT4* and *NANOG* mRNAs decreased dramatically (Fig. 2F). Similarly, when VAL-3 cells were induced to differentiate towards the mesodermal lineage upon AVBF induction, no significant difference in *FOXM1* expression between samples was found (Fig. 2G), although OCT4 and NANOG were significantly downregulated (data not shown).

Taken together, the lack of direct correlation of expression between *FOXM1* and core pluripotency marker genes during VAL-3 differentiation did not support FOXM1 as an upstream regulator of the core pluripotent circuitry in differentiating hESCs. It is interesting to note that *FOXM1* expression is sustained in VAL-3 cells induced to differentiate into the mesodermal and endodermal lineages.

3.3. FOXM1 knockdown have a subtle effect on hESC undifferentiated state

To investigate the functional role of FOXM1 in undifferentiated hESCs, we transiently knocked down FOXM1 in hESCs by RNAi. VAL-3

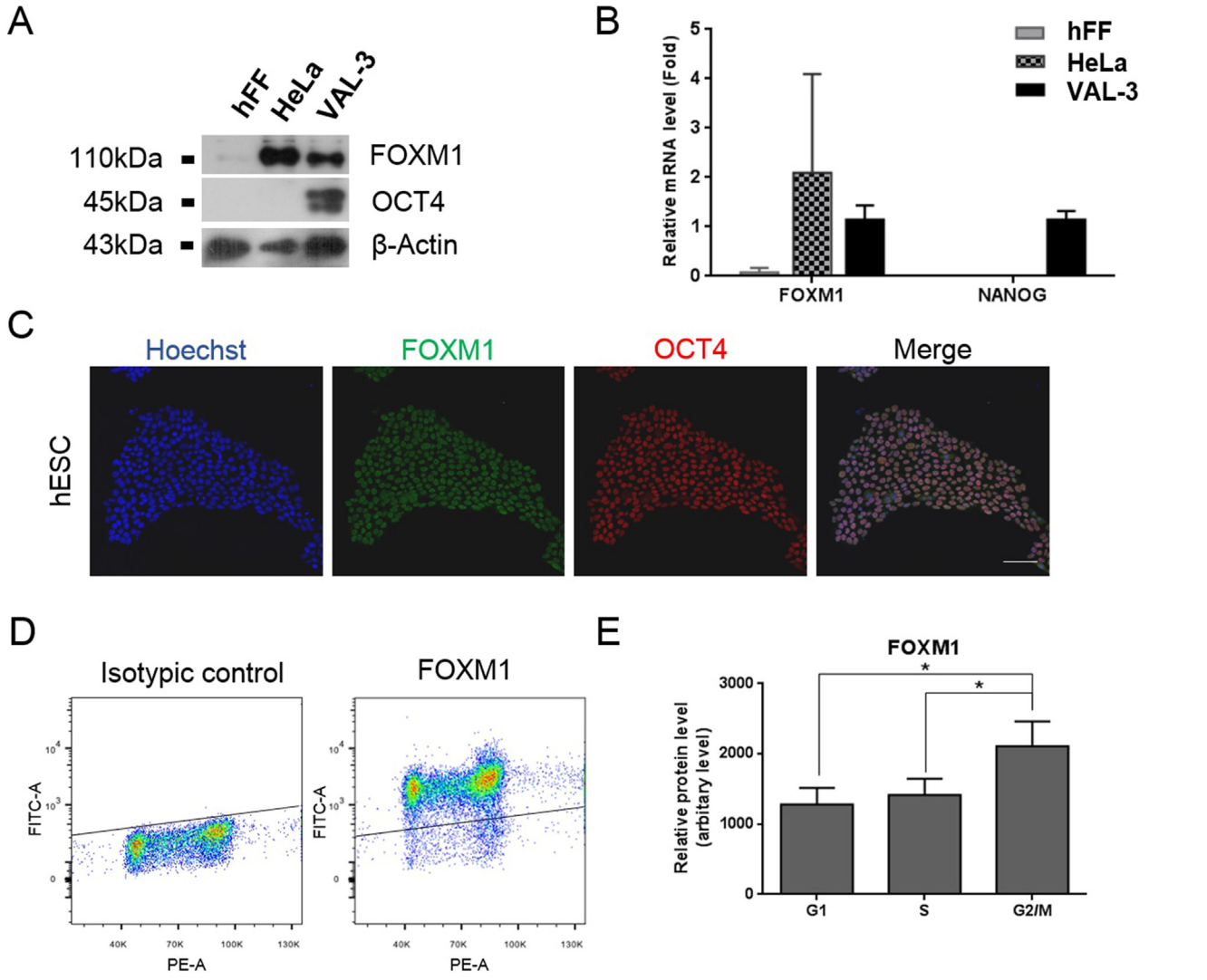

Fig. 1. FOXM1 expression in undifferentiated hESCs. (A–B) Comparing FOXM1 expression in hFF, HeLa and hESC (VAL-3) cells. (A) Immunoblot analysis of cell lysates. (B) Expression of *FOXM1* and *NANOG* determined by qRNA analysis. $n = 3$. (C) Double immunofluorescence staining of FOXM1 and OCT4 in hESCs. (D–E) Expression of FOXM1 in hESCs across different cell cycle phases was examined by bivariate flow cytometric analysis. (D) FOXM1-positive cells (above the straight line) were gated as those with FITC intensity higher than the background (set by the isotypic control). Data shown are representative of four biological replicates. (E) Graphic representation of FOXM1 expression levels at different cell cycle phases. The FOXM1-positive population was gated into three subpopulations (G1, S and G2/M) based on DNA content. Values are presented as the mean FITC intensity of different subpopulations ± SEM. $^{*}P < 0.05$. $n = 4$.

cells were transfected with either FOXM1-targeting siRNAs [#1 or #2 previously validated (Kong et al., 2013; Liu et al., 2013)] or non-specific control siRNA. Transfection of FOXM1 siRNA #1 and #2 led to >70% suppression of FOXM1 mRNA levels compared to control siRNA at 72 h post-transfection, with siRNA #2 showing stronger suppressive effect (Fig. 3A). Depletion of FOXM1 at protein level by both FOXM1 siRNAs was verified by immunoblot analysis (Fig. 3B). The FOXM1 siRNAs used in our knockdown study depleted expression of the A, B and C isoforms of FOXM1 and the qPCR assay was designed to detect the mRNA expression of all three isoforms. Because FOXM1 was reported to be essential for pluripotency in mouse ES cells (Tan et al., 2014), we first examined the effect of FOXM1 knockdown on VAL-3 colony morphology. Unlike mouse ES cells, FOXM1-depleted VAL-3 cells did not show morphological changes suggestive of differentiation. Although the colonies appeared smaller, cells remained closely packed (Supplementary Fig. 3). Next, we determined the effect of FOXM1 depletion on the expression of core pluripotent marker genes using qPCR. Despite a transient reduction of *OCT4* and *NANOG* mRNA levels after transfection with FOXM1 siRNA #2 (which showed a stronger suppressive effect) for two days, expression of *OCT4*, *NANOG* and *SOX2* stayed high in FOXM1-depleted VAL-3 cells on day 3 and day 4 after transfection (Fig. 3C–E). Expression of the early differentiation marker gene *KRT18* was not induced after FOXM1 knockdown (Fig. 3F). Intriguingly, we observed the induced expression of differentiation marker SSEA-1 by immunofluorescence in FOXM1-depleted cells (Supplementary Fig. 4). Taken together, the findings suggested that transient FOXM1 depletion does not induce rapid loss of the undifferentiated state of hESCs.

3.4. FOXM1 knockdown impairs hESC proliferation

The smaller colony size of VAL-3 cells upon FOXM1 knockdown suggested slowdown in hESC proliferation. To address this notion, VAL-3 cells transfected with FOXM1 siRNA #2 or control siRNA were monitored for growth using the NF proliferation assay. FOXM1 depletion led to significant reduction in cell number on day 4 after transfection, indicating impaired cell proliferation and/or survival of hESCs (Fig. 4A). To assess cell cycle kinetics upon FOXM1 knockdown, we examined the cell cycle profile of transfected VAL-3 cells using flow cytometric analysis. Interestingly, FOXM1 depletion resulted in an increase in the percentage of cells at G2/M phase (average increase of

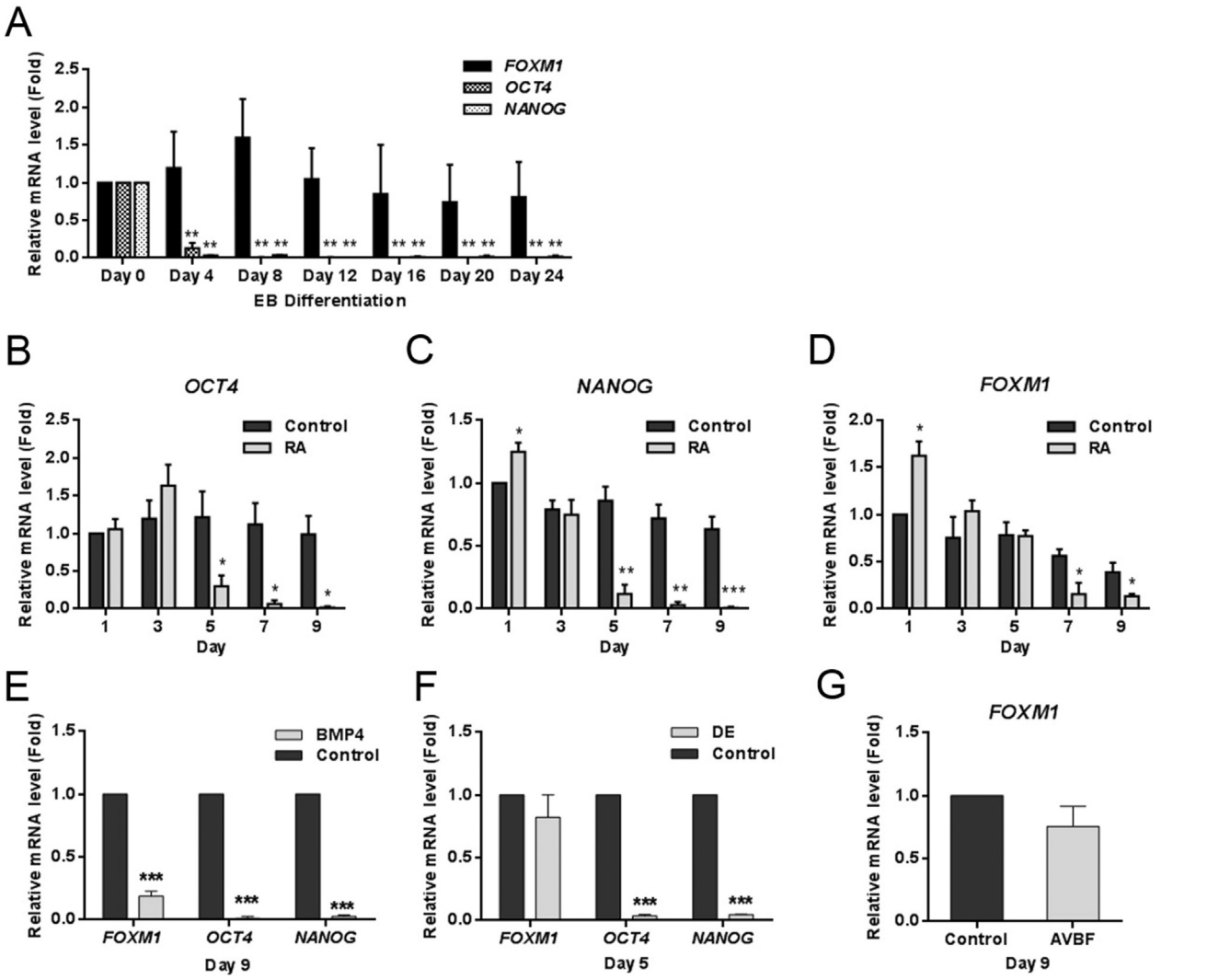

Fig. 2. Expression of *FOXM1* in hESCs undergoing spontaneous and induced differentiation. Expression of *FOXM1* and the pluripotent markers *OCT4* and *NANOG* was determined by qPCR analysis and shown as mean ± SEM. (A) Differentiation as embryoid bodies (EBs). $^{**}P < 0.01$ compared with day 0. $n = 4$. (B–D) Retinoid acid (RA)-induced differentiation. hESCs were induced to differentiate by incubating with 5 μM RA, while control cells were incubated with bFGF. Gene expression levels in control samples on day 1 were taken as reference. $^{*}P < 0.05$, $^{**}P < 0.01$ when compared with bFGF control of corresponding day. $n = 4$. (E–G) Expression of *FOXM1*, *OCT4* and *NANOG* in differentiated hESCs. hESCs were induced to differentiate using BMP4 for nine days (E), using definitive endoderm differentiation (DE) kit reagents for five days (F), and using AVBF treatment for nine days (G). Control samples were treated with bFGF instead of morphogens. Gene expression levels in control samples on day 1 were taken as reference. $^{***}P < 0.001$ when compared with bFGF control of corresponding day. $n = 3$.

8%, $P < 0.05$), while the percentage of cells in S phase showed a trend of reduction (Fig. 4B and C). Cell proportion in G1 phase showed no significant difference (Fig. 4B and C). The sub-G1 population did not increase, ruling out cell death as the cause of the cell number decrease.

To determine whether the increase in G2/M percentage is due to a slowdown of mitosis, we assayed the proportion of cells positive for the phosphorylation of histone H3 at Ser10 (PH3), an established mitotic marker (Hans and Dimitrov, 2001), using immunofluorescence (Fig. 4D). Importantly, cell counting indicated a significant increase in the percentage of cells positive for PH3 in the FOXM1-depleted group compared with control (Fig. 4E). After analyzing the number of mitotic cells in each sub-stage of mitosis (prophase, prometaphase, metaphase/anaphase/telophase) based on the staining pattern of chromosomes, the overall increase in the proportion of PH3 positive cells could be attributed to the accumulation of cells in prophase and metaphase/anaphase/telophase (Fig. 4E). Notably, we occasionally observed misaligned chromosomes along the equator during mitosis in FOXM1-depleted cells (Fig. 4F), implying defects incurred during chromosomal segregation at metaphase. Experiments conducted using siRNA #1 gave similar but weaker cell cycle effects (data not shown). Collectively, our findings support an important role for FOXM1 in the regulation of hESC proliferation, in particular M phase progression.

3.5. FOXM1 knockdown sensitizes hESCs to oxidative stress

FOXM1 regulates the intracellular levels of reactive oxygen species (ROS) and protect against oxidative stress through activation of antioxidant enzymes in human cells (Park et al., 2009; Halasi et al., 2013). To investigate the effect of FOXM1 depletion on viability of hESCs under oxidative stress, VAL-3 cells transfected with control or FOXM1 siRNA were incubated with hydrogen peroxide (H_2O_2) at various concentrations for one hour. We observed a significant reduction in cell growth of FOXM1-depleted hESCs, compared with the controls at various H_2O_2 concentrations (Fig. 5A). Notably, the difference in cell number between FOXM1 siRNA- and control siRNA-treated cells increased as H_2O_2 concentration increased (Fig. 5A), implying that FOXM1 depletion rendered hESCs more vulnerable to growth inhibition by oxidative stress. To examine the intracellular ROS level in hESCs depleted of FOXM1, siRNA-transfected VAL-3 cells were loaded with CM-H2DCFDA before incubation in either normal culture medium or medium containing

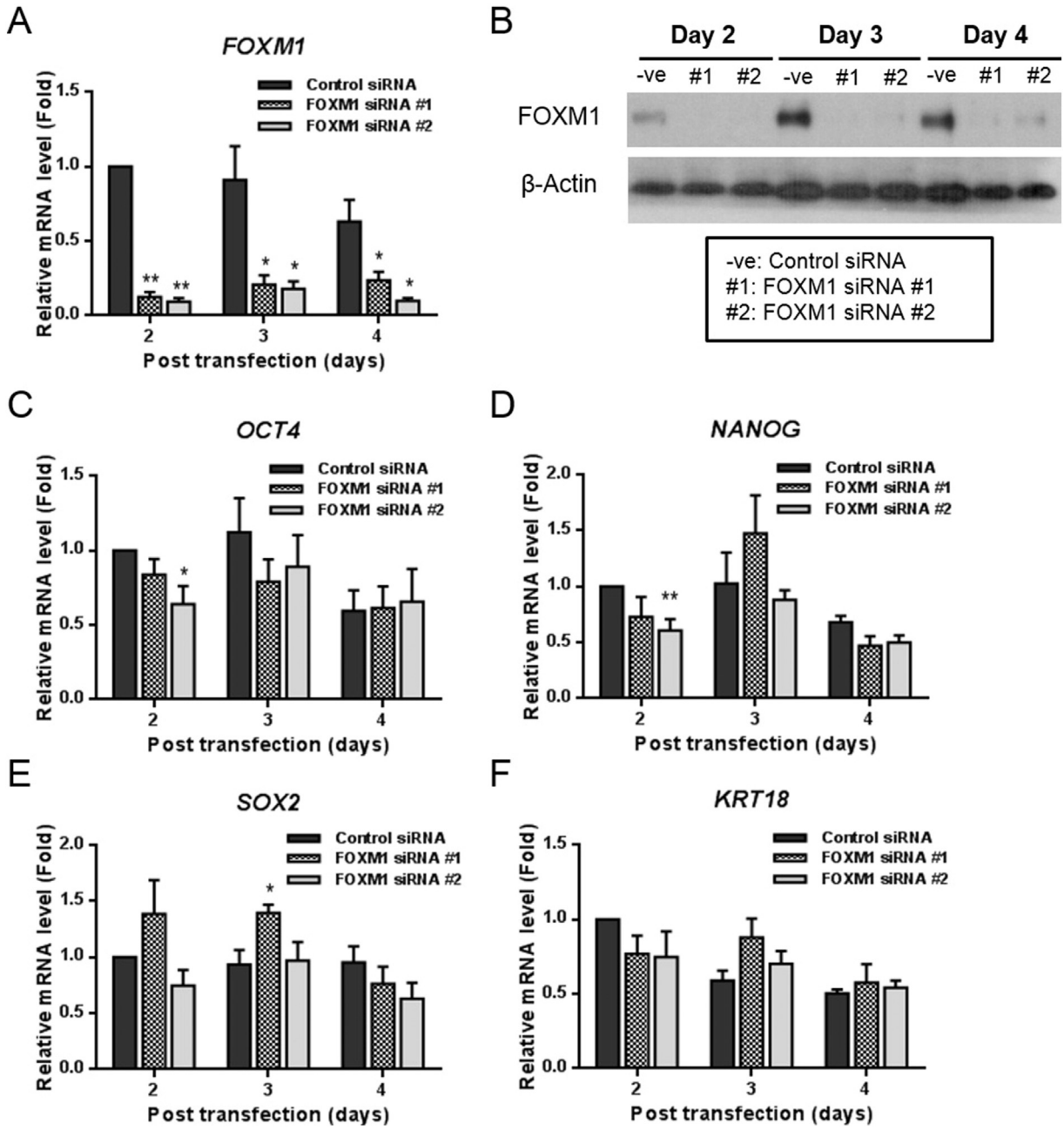

Fig. 3. Depletion of FOXM1 in hESCs by RNA interference does not induce sustainable downregulation of pluripotent genes. hESCs, transfected with either control siRNA, FOXM1 siRNA #1 or siRNA #2, were analyzed at two to four days post-transfection. qPCR analysis was conducted. Expression data shown as mean ± SEM are relative to control samples at day 2 post-transfection. (A–B) Temporal expression of FOXM1 in hESCs after siRNA transfection. (A) FOXM1 siRNA #1 and #2 effectively ablated expression of *FOXM1* in hESCs. $^{*}P < 0.05$, $^{**}P < 0.01$ when compared with control siRNA sample of corresponding day. $n = 4$. (B) Immunoblot analysis showing FOXM1 depletion in hESCs after transfection with FOXM1 siRNA #1 and #2. Data shown are representative of four biological replicates. (C-F) Expression of the pluripotent genes *OCT4* (C), *NANOG* (D), *SOX2* (E) and the early differentiation marker *KRT18* (F) was examined by qPCR in hESCs from two to four days post-transfection. $^{*}P < 0.05$, $^{**}P < 0.01$ when compared with control siRNA sample of corresponding day. $n = 4$.

100 μM H_2O_2 and eventually subjected to quantitative measurement of ROS by flow cytometry. While the intracellular ROS level remained at comparable levels in samples incubated in normal medium, H_2O_2 treatment induced a significant increase in ROS level in FOXM1-depleted cells (Fig. 5B), suggesting a role for FOXM1 in suppressing ROS formation and protecting against oxidative stress. Superoxide dismutase 2 (SOD2) and catalase (CAT), implicated as the dominant antioxidant enzymes in hESCs (Cho et al., 2006), were previously reported as transcriptional targets of FOXM1 (Park et al., 2009). To test whether they are FOXM1 targets in VAL-3 cells, we investigated the expression of *SOD2* and *CAT* at both the RNA and protein levels after depletion of FOXM1 expression by both siRNA #1 and #2. Both qPCR and immunoblot analyses indicated lowered expression of *CAT* but not *SOD2* upon FOXM1 knockdown (Fig. 5C and D). These data suggest that FOXM1 depletion sensitizes hESCs against oxidative stress, possibly through downregulation of the anti-oxidant gene *CAT*.

3.6. Identification of FOXM1 target genes in hESCs

To identify FOXM1 target genes in hESCs on a genome-wide scale, we carried out chromatin immunoprecipitation followed by sequencing (ChIP-seq) using FOXM1 antibody previously employed in similar studies. Our results showed that 1377 FOXM1-bound peaks were identified using MACS (Zhang et al., 2008), with 45% of the peaks located either within 1000 bp of transcription start site (TSS) or in the 5′ untranslated region (UTR) of potential target genes, assigned based on distance

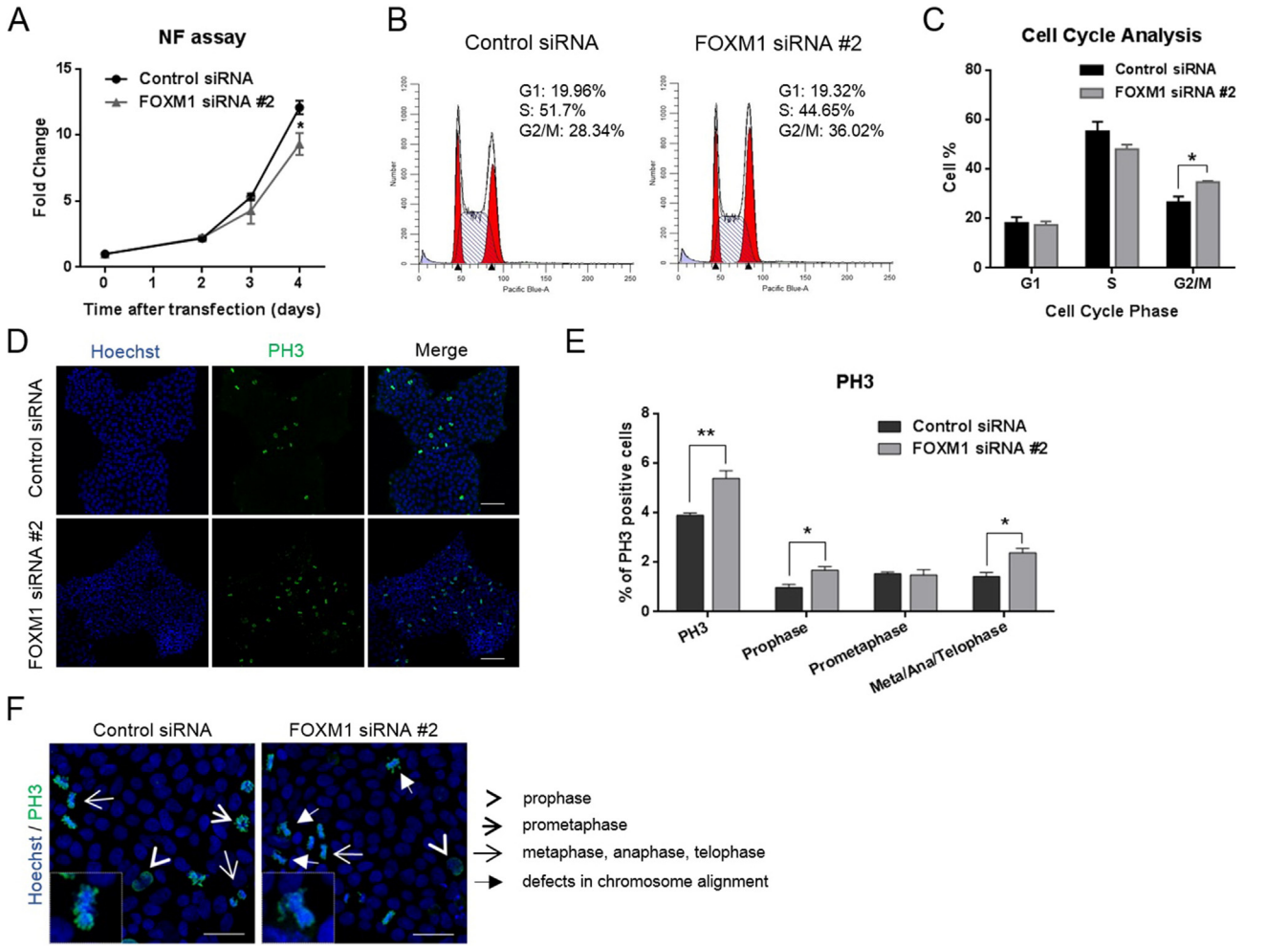

Fig. 4. FOXM1 knockdown in hESCs impairs cell proliferation with delay at the G2/M phase of the cell cycle. (A) Proliferation of hESCs after transfection with control or FOXM1 siRNA #2 was monitored by NF cell proliferation assay for four days. Relative fold change in cell number was expressed with reference to cell number on day 0. Data are shown as mean ± SEM; $^{*}P < 0.05$ when compared with control siRNA sample. $n = 3$. (B) Flow cytometric histograms showing the cell cycle profiles of hESCs transfected with control or FOXM1 siRNA #2 at three days post-transfection. Also shown are the percentages of cells in various cell cycle phases. Data shown are representative of four biological replicates. (C) Quantification of cell cycle distribution revealed an elevated percentage of cells in G2/M phase. Data are shown as mean ± SEM. $^{*}P < 0.05$ when compared with control siRNA sample. $n = 4$. (D–F) Immunofluorescence analysis of the mitotic marker phospho-histone H3 Ser10 (PH3) (green) in hESCs treated with control or FOXM1 siRNA at three days post-transfection. DNA was stained with Hoechst. Scale bar = 100 μm. (E) Quantification of PH3-positive cells and mitotic cells in hESCs treated with control or FOXM1 siRNA at three days post-transfection. Mitotic cells were regarded as in prophase, prometaphase, or metaphase/anaphase/telophase depending on the chromosome staining pattern. Data are shown as mean ± SEM. $^{**}P < 0.01$ when compared to control group. $n = 4$. (F) Images at higher magnification. FOXM1 siRNA #2-treated cells displayed defects in mitosis and chromosome alignment at the equator (enlarged in inset).

(Fig. 6A and Supplementary Table 2). The result of ChIP-seq was validated by ChIP–qPCR analysis on randomly selected FOXM1 binding loci of different peak scores, confirming enriched FOXM1 binding to the putative targets (Supplementary Fig. 5). To establish the biological functions of FOXM1 in relation to transcriptional regulation, we performed Gene Ontology (GO) enrichment analysis for the potential FOXM1 target genes (Huang, 2009a; Huang, 2009b) (Fig. 6B). The most significantly enriched GO terms were associated with cell cycle, chromosome organization and translation. Interestingly, the cluster of enriched GO terms related to cell cycle predominantly attributed to mitotic progression, highlighting the importance of FOXM1 in the regulation of cell cycle progression and mitosis at the transcriptional level.

FOXM1 enrichment was found in the promoter regions of the known target genes *CCNB1* (Leung et al., 2001) and *CDK1* (Chen et al., 2013) (Fig. 6C). A recent study showed that CDK1 is essential to pluripotency and cell cycle progression in hESCs (Neganova et al., 2014). ChIP–qPCR analysis confirmed significant enrichment of FOXM1 binding to these target regions compared to normal IgG control (Fig. 6D). To assess the regulatory function of FOXM1 on these genes, their expression was assayed by qPCR analysis before and after FOXM1 knockdown using FOXM1 siRNA #2. Expression of *CCNB1* ($P < 0.001$) and *CDK1* ($P < 0.05$) was significantly reduced on day 3 post-transfection (Fig. 6E). Interestingly, examination of the ChIP-seq binding peaks also revealed enrichment of FOXM1 binding at the promoter of *OCT4* in undifferentiated VAL-3 cells (Supplementary Fig. 6).

To probe *cis* elements facilitating FOXM1-chromatin interactions in hESCs, we performed motif enrichment analysis to look for overrepresented DNA motifs using MEME (Bailey and Elkan, 1994). Their matching with known motifs using TOMTOM (Gupta et al., 2007) revealed enrichment of the binding motifs of ZBTB33, TP53 and PRDM14 (Fig. 6F). While ZBTB33 and TP53 binding motifs were previously associated with FOXM1 chromatin binding (Choudhary et al., 2015), it is surprising to see the binding motif of PRDM14, which was shown to be essential to the regulation of pluripotency in hESCs (Chia et al., 2010; Chan et al., 2013). Similar motif identification results were obtained using another algorithm DREME. Intriguingly, the canonical

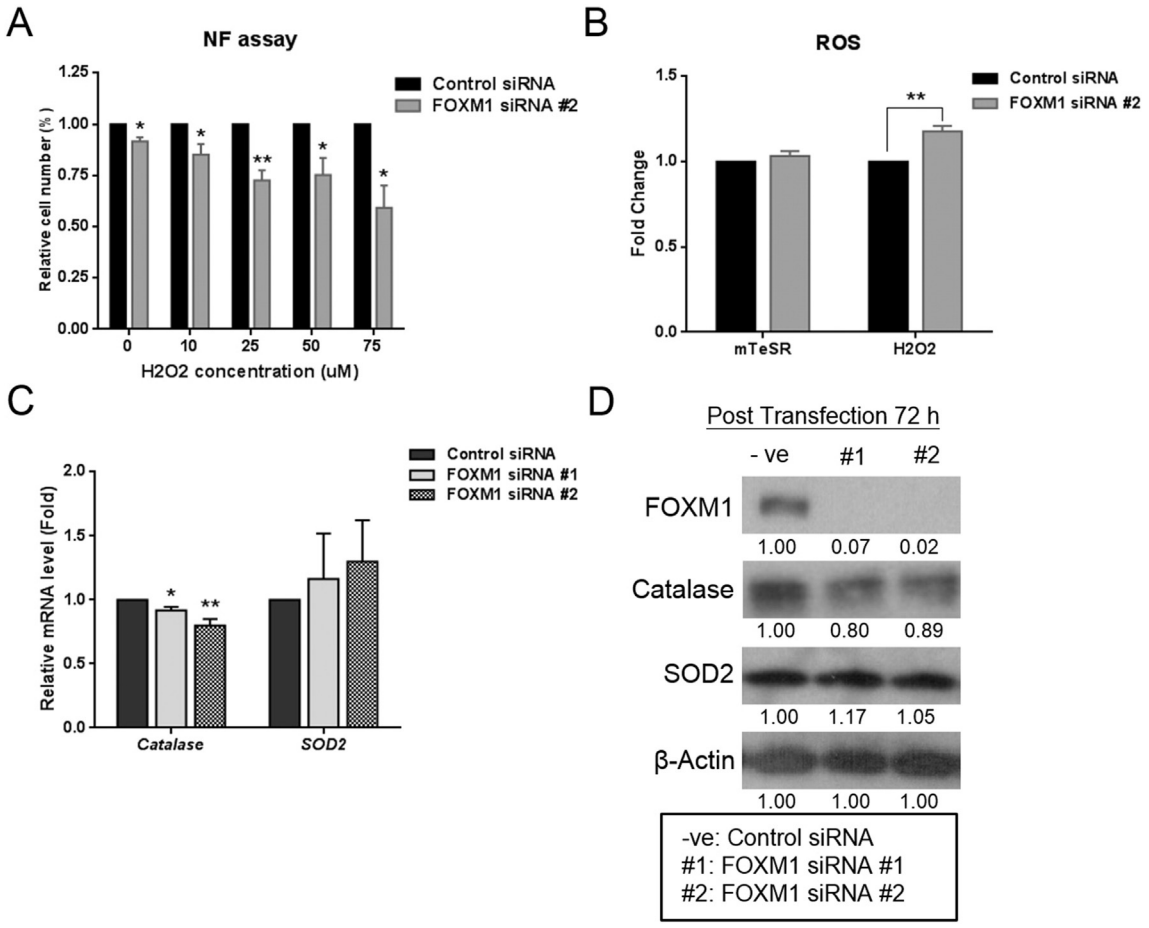

Fig. 5. FOXM1 knockdown sensitizes hESCs to oxidative stress. (A) Growth of hESCs, transfected with control or FOXM1 siRNA #2 and then treated with H_2O_2 for one hour at various concentrations, was determined by NF cell proliferation assay. Data are shown as mean ± SEM. $^*P < 0.05$,$^{**}P < 0.01$ when compared to control sample at the corresponding H_2O_2 concentration. $n = 3$. (B) Relative ROS level in hESCs transfected with control or FOXM1 siRNA three days post-transfection. Cells were loaded with CM-H2DCFDA prior to incubation in mTeSR with or without 100 μM H_2O_2. Data are shown as mean ± SEM. $^{**}P < 0.01$ when compared to control sample. $n = 3$. (C) Expression of *CAT* and *SOD2* transcript levels in hESCs was analyzed by qPCR upon FOXM1 knockdown at 72 h post-transfection. Data are shown as mean ± SEM. $^*P < 0.05$, $^{**}P < 0.01$ when compared to control sample. $n = 3$. (D) Immunoblot analysis of CAT and SOD2 expression in hESCs transfected with control or FOXM1 siRNAs at 72 h post-transfection. Data shown are representative of three biological replicates.

forkhead binding motif was not significantly enriched in the present peak set, supporting the notion that chromatin recruitment of FOXM1 in the human genome is mediated mainly via binding to non-canonical DNA sequences (Sanders et al., 2015).

Most recently, ChIP-seq analysis of FOXM1 binding was conducted using early differentiating retinal pigment epithelium (RPE) cells derived from the hESC line SHEF1 (Choudhary et al., 2015), and this peak set identifies FOXM1 binding sites in the genome of non-cancerous cells. Importantly, comparing our peak set in undifferentiated hESCs against the early differentiating RPE dataset revealed extensive overlap of FOXM1 targets. Out of the 1377 high coverage FOXM1 binding peaks in VAL-3 cells, 498 peaks (36.2%) were commonly occupied by FOXM1 in RPE cells to give 506 overlapped regions, indicating a significant degree of overlap in chromatin binding profiles (Fig. 6G). In contrast, comparison of FOXM1 binding peaks between VAL-3 cells and OE33 cells derived from human oesophageal adenocarcinoma (Wiseman et al., 2015) showed only 67 shared binding peaks (4.9%) to give 73 overlapped regions, suggesting a considerable difference in the chromatin binding profile of FOXM1 between hESCs and cancer cells (Fig. 6G). It is worth noting that the peak and region numbers differ as some peaks in one dataset were found to overlap with two peaks in another dataset to generate two regions. Representative views of the peaks that are shared and different between VAL-3 and RPE/OE33 are shown in Supplementary Fig. 7. Importantly, the well-established G2/M phase expressed target genes CCNB1 and CENPF are within the regions shared by VAL-3 and OE33 (Supplementary Table 3). However, these regions are not shared by RPE, which was derived from early differentiating hESCs.

4. Discussion

FOXM1 has been extensively studied in cancer cells and during mouse development and shown to play a role in a broad spectrum of biological processes. The first link of FOXM1 to the regulation of stem cell pluripotency came with the demonstration that FOXM1 acted through the core pluripotent circuitry to mediate the maintenance of pluripotency and self-renewal in mouse pluripotent cells (Xie et al., 2010; Tan et al., 2014). This notion was further strengthened when FOXM1 knockdown was shown to downregulate *OCT4* expression in human EC cells (Chen et al., 2015), but the functional relevance of FOXM1 in hESC remain unclear.

In this study, we showed that FOXM1 was highly expressed in undifferentiated hESCs. Similar to other cell types (Korver et al., 1997b; Leung et al., 2001; Laoukili et al., 2008), FOXM1 displayed periodic expression during the cell cycle with heightened levels at G2/M. FOXM1 levels did not decrease precipitously like the core pluripotent markers but showed fluctuations in spontaneously differentiating VAL-3 cells. Due to the random nature of spontaneous differentiation, EBs consist of a mix of cells committing to various lineages (Pekkanen-Mattila et al., 2010). The fluctuating expression of FOXM1 during EB differentiation suggests

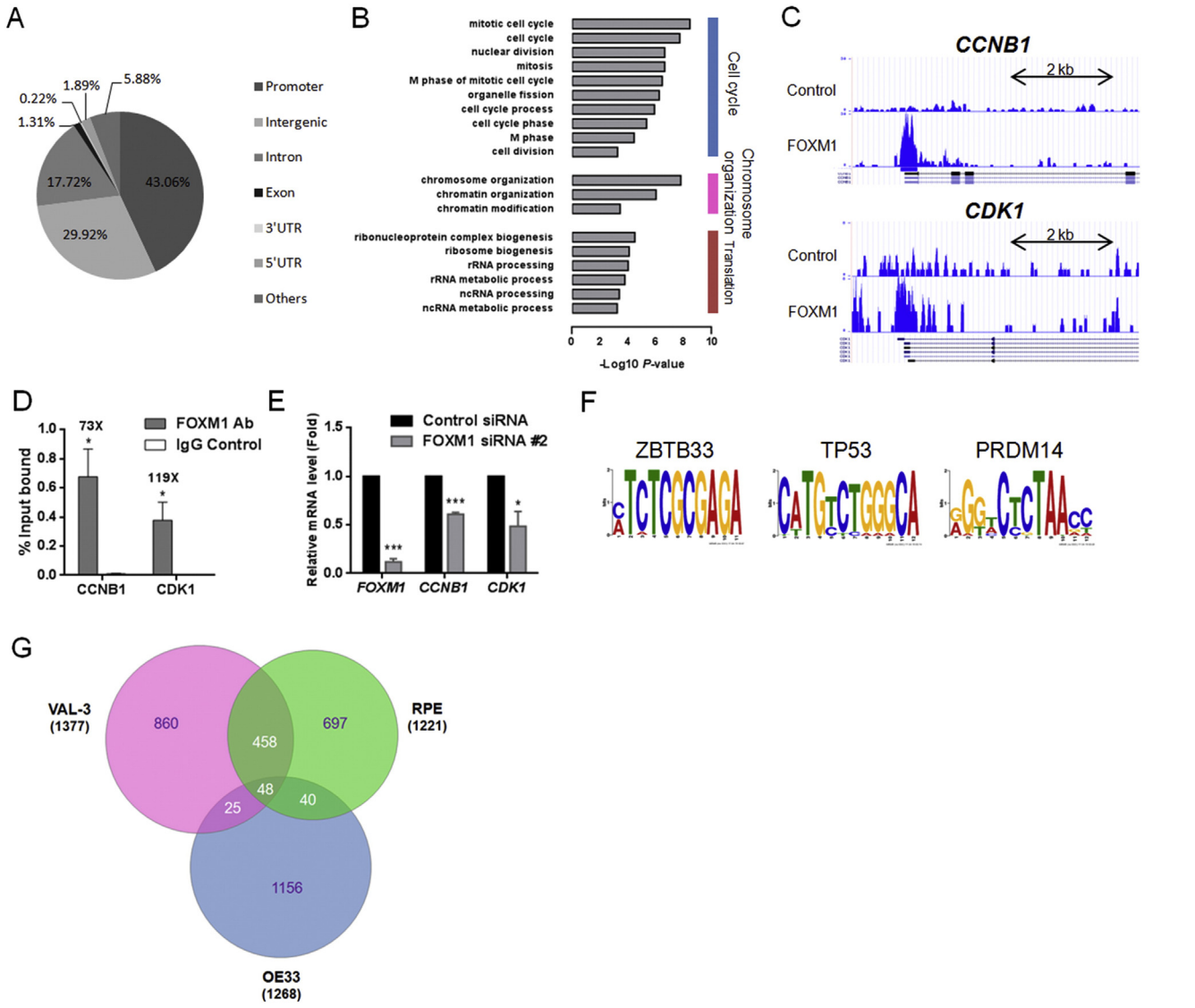

Fig. 6. Genome-wide analysis of FOXM1 binding in hESCs. (A) Genomic distribution of FOXM1 binding regions in VAL-3 cells. (B) Gene Ontology enrichment analysis of FOXM1 binding targets. (C) Peaks of FOXM1 binding at the promoters of *CCNB1* and *CDK1*. (D) Preferential association of FOXM1 with *CCNB1* and *CDK1* promoters. ChIP–qPCR analysis was performed using primers specific to the corresponding promoter sequences and the percentage enrichment shown relative to input as mean ± SEM. $^{*}P < 0.05$ when compared with IgG control. $n = 3$. (E) Expression of *FOXM1*, *CCNB1* and *CDK1* in hESCs transfected with control or FOXM1 siRNA #2 was analyzed by qPCR at day 3 post-transfection. Data are shown as mean ± SEM. $^{***}P < 0.001$, $^{*}P < 0.05$ when compared with control siRNA sample. $n = 3$. (F) Motif enrichment analysis of FOXM1 binding regions identified motifs recognized by ZBTB33, TP53 and PRDM14. (G) Venn diagram showing the overlap of FOXM1 binding peaks (numbers in purple) to give overlapped binding regions (numbers in white) in VAL-3, RPE and OE33 cells.

that FOXM1 expression/function may be required in certain lineage differentiation pathways but does not necessarily correlate with the undifferentiated state of hESCs. Indeed, in vitro differentiation of VAL-3 cells induced by various morphogens gave different outcomes. While downregulation was observed in differentiating hESCs upon RA and BMP4 induction, FOXM1 expression was sustained following differentiation driven by AVBF (mesodermal) and a definitive endoderm differentiation kit. The functional requirement of FOXM1 during differentiation into mesodermal and endodermal derivatives requires further investigation. Our findings do not support the direct regulation of pluripotent genes by FOXM1 during hESC differentiation, in contrast to previous findings in mouse and human EC cells (Xie et al., 2010; Chen et al., 2015).

In line with the differentiation experiments, siRNA-mediated knockdown of FOXM1 in hESCs did not induce rapid loss of undifferentiated state or substantial downregulation of the core pluripotent markers. Our data differ from the rapid loss of the undifferentiated state and downregulation of *OCT4* and *NANOG* upon FOXM1 knockdown in mouse pluripotent cells (Xie et al., 2010; Tan et al., 2014). FOXM1 binds to the *OCT4* promoter, stimulating its expression in both mouse and human EC cells (Xie et al., 2010; Chen et al., 2015). Interestingly, we did observe subtle and transient downregulation of *OCT4* and *NANOG* in VAL-3 cells two days after FOXM1 siRNA transfection, as well as induced expression of SSEA-1, indicating signs of differentiation upon FOXM1 knockdown. Further, enrichment of FOXM1 binding at the promoter of *OCT4* suggests that FOXM1 might participate in the transcriptional regulation of *OCT4*. The subtle and transient effect observed in our study may be due to compensatory regulation upon FOXM1 knockdown. Interestingly, one of the top enriched binding motifs that coexists with FOXM1 binding is recognized by PRDM14, which was recently shown to be essential to pluripotency through interactions with PRC2 to establish repressive histone modifications and suppress differentiation genes in hESCs (Chia et al., 2010; Chan et al., 2013). Potential interactions between FOXM1 and PRDM14 may be specific

to hESCs and highlight a possible link of FOXM1 to pluripotency through a mechanism other than direct transcriptional control of the core pluripotent genes.

Based on the differentiation and siRNA studies reported here, the mechanistic regulation of FOXM1 towards pluripotency control and differentiation might differ between mouse and human ES cells. The discrepancy can be attributed to the different developmental status of human versus mouse ES cells (Nichols and Smith, 2009; Pera and Tam, 2010). On the other hand, despite being pluripotent the EC cells have adapted towards tumor growth via suppression of differentiation, and are distinctly different from ES cells (Sperger et al., 2003; Andrews et al., 2005). In EC cells there are additional copies of chromosome 12p (Andrews et al., 2005), where *FOXM1* is located (Korver et al., 1997a). Given that FOXM1 is over-expressed in EC cells (Sperger et al., 2003), FOXM1 may regulate a different set of biological pathways (see below), explaining the discrepancy observed.

Human ESCs undergo rapid proliferation with uniquely abbreviated cell cycles to maintain self-renewal and pluripotent capacity (Ruiz et al., 2011; Hindley and Philpott, 2013). The underlying molecular regulation is believed to be distinct from somatic cells (Ruiz et al., 2011; Hindley and Philpott, 2013). In this study, we demonstrated that FOXM1 knockdown led to impairment of hESC proliferation, mainly due to delayed progression through the G2/M phase of the cell cycle accompanied by chromosome abnormalities during mitosis. The G2/M delay with FOXM1 knockdown is consistent with the known function of FOXM1 reported in other mouse and human cell lines (Laoukili et al., 2005; Wang et al., 2005; Wonsey and Follettie, 2005). It is also reminiscent of the arrest in G2 phase and accumulation of cells in mitosis after CDK1 knockdown recently reported in hESCs (Neganova et al., 2014).

The critical role of FOXM1 in mitosis in hESCs is supported by the enrichment of cell cycle genes (in particular M phase relevant genes) in the GO analysis of the potential FOXM1 target genes discovered in the ChIP-seq analysis. We confirmed that the known FOXM1 direct targets *CDK1* and *CCNB1* are also downstream targets of FOXM1 in hESCs based on their downregulation upon FOXM1 knockdown and association of FOXM1 with their promoters. In somatic cells, FOXM1 is phosphorylated and activated by the CDK1/CCNB1 complex at the S/G2 phase transition (Chen et al., 2009). FOXM1 might also work synergistically with CDK1 and CCNB1 in a positive feedback manner to promote timely progression through G2/M phase in hESCs. CDK1 depletion showed more obvious effect on hESC pluripotency (Neganova et al., 2014) than FOXM1 knockdown reported here. This might be attributed to the incomplete suppression of CDK1 function upon FOXM1 knockdown and there may also be compensatory regulation of CDK1 upon FOXM1 depletion.

Human ESCs exhibit higher resistance to H_2O_2-induced stress compared to their differentiated counterparts (George et al., 2009) by having an efficient repair capacity with elevated expression of DNA repair genes (Maynard et al., 2008). Our study supports the involvement of FOXM1 in the defense mechanism of hESCs against oxidative stress. FOXM1 knockdown impaired recovery of hESCs following H_2O_2 treatment, as evidenced by elevated ROS level and reduced cell growth, indicating that FOXM1 depletion renders hESCs more vulnerable to oxidative stress. FOXM1 depletion was accompanied by downregulation of *CAT* but not *SOD2* at both the RNA and protein levels, supporting a role for CAT in the defense mechanism. However, no significant binding of FOXM1 to the proximal promoter region of *CAT* (~10 kb upstream) was detected by ChIP-seq and ChIP analysis (data not shown). It remains to be tested whether FOXM1 regulates *CAT* transcription by binding to sites far away or whether FOXM1 mediates its protective effect via other target genes.

The significant overlap of potential FOXM1 targets between VAL-3 (reported here) and RPE cells points to a core set of targets regulated by FOXM1 in non-cancerous cells with healthy genomes. In fact, ZBTB33 and TP53 are the top two binding motifs coexisting with FOXM1-bound sequences in both data sets (Choudhary et al., 2015). Unexpectedly, the VAL-3 peak set overlaps with relatively less targets identified in the cancer cell line OE33. The overexpression of FOXM1 and thereby the deregulation of downstream targets in various cancer cells contributes to its principal regulatory role throughout tumorigenesis, including tumor initiation, invasion and metastasis (Wierstra, 2013a). The disparate FOXM1 chromatin binding profile may imply that FOXM1 orchestrates very different sets of downstream targets in non-cancerous cells versus cancer cells, which are subjected to regulation by very different signaling pathways. Thus, further investigation is warranted to differentiate the molecular mechanisms underscoring FOXM1 regulation in normal healthy cells and transformed cells to understand its regulatory roles in diverse biological processes, which is of therapeutic relevance for targeting cancer cells.

5. Conclusion

In summary, we provided the first evidence that FOXM1 plays an important role in the maintenance of cell proliferation in the hESC cell line VAL-3, with significant functions in safe-guarding progression through G2/M phase mediated by the transcriptional regulation of cell cycle genes including *CCNB1* and *CDK1*. FOXM1 also protected hESCs against oxidative stress. Further study of FOXM1 in the context of hESCs will provide interesting insights into the unique control of abbreviated cell cycle proliferation and pluripotency in non-cancerous cells, which is critical for the manipulation and differentiation of hESCs required in regenerative medicine.

Supplementary data to this article can be found online at http://dx.doi.org/10.1016/j.scr.2016.03.007.

Acknowledgment

This work was supported by a grant from the Hong Kong Research Grants Council (N_HKU 763/11), in consultation with the National Natural Science Foundation of China, awarded to K.-M. Y.

References

Andrews, P.W., Matin, M.M., Bahrami, A.R., Damjanov, I., Gokhale, P., Draper, J.S., 2005. Embryonic stem (ES) cells and embryonal carcinoma (EC) cells: opposite sides of the same coin. Biochem. Soc. Trans. 33 (Pt 6), 1526–1530.

Arduini, B.L., Brivanlou, A.H., 2012. Modulation of FOXD3 activity in human embryonic stem cells directs pluripotency and paraxial mesoderm fates. Stem Cells 30 (10), 2188–2198. http://dx.doi.org/10.1002/stem.1200.

Bailey, T.L., 2011. DREME: motif discovery in transcription factor ChIP-seq data. Bioinformatics 27 (12), 1653–1659. http://dx.doi.org/10.1093/bioinformatics/btr261.

Bailey, T.L., Elkan, C., 1994. Fitting a mixture model by expectation maximization to discover motifs in biopolymers. Proc. Int. Conf. Intell. Syst. Mol. Biol. 2, 28–36.

Becker, K.A., Ghule, P.N., Therrien, J.A., Lian, J.B., Stein, J.L., van Wijnen, A.J., Stein, G.S., 2006. Self-renewal of human embryonic stem cells is supported by a shortened G1 cell cycle phase. J. Cell. Physiol. 209 (3), 883–893. http://dx.doi.org/10.1002/jcp.20776.

Boyer, L.A., Lee, T.I., Cole, M.F., Johnstone, S.E., Levine, S.S., Zucker, J.P., ... Young, R.A., 2005. Core transcriptional regulatory circuitry in human embryonic stem cells. Cell 122 (6), 947–956. http://dx.doi.org/10.1016/j.cell.2005.08.020.

Bramswig, N.C., Everett, L.J., Schug, J., Dorrell, C., Liu, C., Luo, Y., ... Kaestner, K.H., 2013. Epigenomic plasticity enables human pancreatic alpha to beta cell reprogramming. J. Clin. Invest. 123 (3), 1275–1284. http://dx.doi.org/10.1172/jci66514.

Chan, Y.S., Goke, J., Lu, X., Venkatesan, N., Feng, B., Su, I.H., Ng, H.H., 2013. A PRC2-dependent repressive role of PRDM14 in human embryonic stem cells and induced pluripotent stem cell reprogramming. Stem Cells 31 (4), 682–692. http://dx.doi.org/10.1002/stem.1307.

Chen, Y.J., Dominguez-Brauer, C., Wang, Z., Asara, J.M., Costa, R.H., Tyner, A.L., ... Raychaudhuri, P., 2009. A conserved phosphorylation site within the forkhead domain of FoxM1B is required for its activation by cyclin-CDK1. J. Biol. Chem. 284 (44), 30695–30707. http://dx.doi.org/10.1074/jbc.M109.007997.

Chen, A.C., Lee, Y.L., Hou, D.Y., Fong, S.W., Peng, Q., Pang, R.T., ... Yeung, W.S., 2012. Study of transforming growth factor alpha for the maintenance of human embryonic stem cells. Cell Tissue Res. 350 (2), 289–303. http://dx.doi.org/10.1007/s00441-012-1476-7.

Chen, X., Muller, G.A., Quaas, M., Fischer, M., Han, N., Stutchbury, B., ... Engeland, K., 2013. The forkhead transcription factor FOXM1 controls cell cycle-dependent gene expression through an atypical chromatin binding mechanism. Mol. Cell. Biol. 33 (2), 227–236. http://dx.doi.org/10.1128/MCB.00881-12.

Chen, Y., Meng, L., Yu, Q., Dong, D., Tan, G., Huang, X., Tan, Y., 2015. The miR-134 attenuates the expression of transcription factor FOXM1 during pluripotent NT2/D1

embryonal carcinoma cell differentiation. Exp. Cell Res. 330 (2), 442–450. http://dx.doi.org/10.1016/j.yexcr.2014.10.022.
Chia, N.Y., Chan, Y.S., Feng, B., Lu, X., Orlov, Y.L., Moreau, D., ... Ng, H.H., 2010. A genome-wide RNAi screen reveals determinants of human embryonic stem cell identity. Nature 468 (7321), 316–320. http://dx.doi.org/10.1038/nature09531.
Cho, Y.M., Kwon, S., Pak, Y.K., Seol, H.W., Choi, Y.M., do J., Park, ... Lee, H.K., 2006. Dynamic changes in mitochondrial biogenesis and antioxidant enzymes during the spontaneous differentiation of human embryonic stem cells. Biochem. Biophys. Res. Commun. 348 (4), 1472–1478. http://dx.doi.org/10.1016/j.bbrc.2006.08.020.
Choudhary, P., Dodsworth, B.T., Sidders, B., Gutteridge, A., Michaelides, C., Duckworth, J.K., ... Benn, C.L., 2015. A FOXM1 dependent mesenchymal–epithelial transition in retinal pigment epithelium cells. PLoS One 10 (6), e0130379. http://dx.doi.org/10.1371/journal.pone.0130379.
George, S., Heng, B.C., Vinoth, K.J., Kishen, A., Cao, T., 2009. Comparison of the response of human embryonic stem cells and their differentiated progenies to oxidative stress. Photomed. Laser Surg. 27 (4), 669–674. http://dx.doi.org/10.1089/pho.2008.2354.
Golos, T.G., Pollastrini, L.M., Gerami-Naini, B., 2006. Human embryonic stem cells as a model for trophoblast differentiation. Semin. Reprod. Med. 24 (5), 314–321. http://dx.doi.org/10.1055/s-2006-952154.
Gudas, L.J., Wagner, J.A., 2011. Retinoids regulate stem cell differentiation. J. Cell. Physiol. 226 (2), 322–330. http://dx.doi.org/10.1002/jcp.22417.
Gupta, S., Stamatoyannopoulos, J., Bailey, T., Noble, W., 2007. Quantifying similarity between motifs. Genome Biol. 8 (2), R24.
Halasi, M., Pandit, B., Wang, M., Nogueira, V., Hay, N., Gartel, A.L., 2013. Combination of oxidative stress and FOXM1 inhibitors induces apoptosis in cancer cells and inhibits xenograft tumor growth. Am. J. Pathol. 183 (1), 257–265. http://dx.doi.org/10.1016/j.ajpath.2013.03.012.
Hans, F., Dimitrov, S., 2001. Histone H3 phosphorylation and cell division. Oncogene 20 (24), 3021–3027. http://dx.doi.org/10.1038/sj.onc.1204326.
Heinz, S., Benner, C., Spann, N., Bertolino, E., Lin, Y.C., Laslo, P., ... Glass, C.K., 2010. Simple combinations of lineage-determining transcription factors prime cis-regulatory elements required for macrophage and B cell identities. Mol. Cell 38 (4), 576–589. http://dx.doi.org/10.1016/j.molcel.2010.05.004.
Hindley, C., Philpott, A., 2013. The cell cycle and pluripotency. Biochem. J. 451 (2), 135–143. http://dx.doi.org/10.1042/BJ20121627.
Huang, D.W., Sherman, B.T., Lempicki, R.A., 2009a. Bioinformatics enrichment tools: paths toward the comprehensive functional analysis of large gene lists. Nucleic Acids Res. 37 (1), 1–13. http://dx.doi.org/10.1093/nar/gkn923.
Huang, D.W., Sherman, B.T., Lempicki, R.A., 2009b. Systematic and integrative analysis of large gene lists using DAVID bioinformatics resources. Nat. Protoc. 4 (1), 44–57. http://dx.doi.org/10.1038/nprot.2008.211.
Jagtap, S., Meganathan, K., Wagh, V., Natarajan, K., Hescheler, J., Sachinidis, A., 2013. All-trans retinoic acid and basic fibroblast growth factor synergistically direct pluripotent human embryonic stem cells to extraembryonic lineages. Stem Cell Res. 10 (2), 228–240. http://dx.doi.org/10.1016/j.scr.2012.12.002.
Kong, X., Li, L., Li, Z., Le, X., Huang, C., Jia, Z., ... Xie, K., 2013. Dysregulated expression of FOXM1 isoforms drives progression of pancreatic cancer. Cancer Res. 73 (13), 3987–3996. http://dx.doi.org/10.1158/0008-5472.can-12-3859.
Korver, W., Roose, J., Clevers, H., 1997a. The winged-helix transcription is expressed in cycling cells. Nucleic Acids Res. 25 (9), 1715–1719.
Korver, W., Roose, J., Wilson, A., Clevers, H., 1997b. The winged-helix transcription factor trident is expressed in actively dividing lymphocytes. Immunobiology 198 (1–3), 157–161. http://dx.doi.org/10.1016/s0171-2985(97)80036-8.
Langmead, B., Trapnell, C., Pop, M., Salzberg, S.L., 2009. Ultrafast and memory-efficient alignment of short DNA sequences to the human genome. Genome Biol. 10 (3), R25. http://dx.doi.org/10.1186/gb-2009-10-3-r25.
Laoukili, J., Kooistra, M.R., Bras, A., Kauw, J., Kerkhoven, R.M., Morrison, A., ... Medema, R.H., 2005. FoxM1 is required for execution of the mitotic programme and chromosome stability. Nat. Cell Biol. 7 (2), 126–136. http://dx.doi.org/10.1038/ncb1217.
Laoukili, J., Stahl, M., Medema, R.H., 2007. FoxM1: at the crossroads of ageing and cancer. Biochim. Biophys. Acta 1775 (1), 92–102. http://dx.doi.org/10.1016/j.bbcan.2006.08.006.
Laoukili, J., Alvarez-Fernandez, M., Stahl, M., Medema, R.H., 2008. FoxM1 is degraded at mitotic exit in a Cdh1-dependent manner. Cell Cycle 7 (17), 2720–2726 (7:17, 2720-2726; 1).
Leung, T.W.C., Lin, S.S.W., Tsang, A.C.C., Tong, C.S.W., Ching, J.C.Y., Leung, W.Y., ... Yao, K.M., 2001. Over expression of FoxM1 stimulates cyclinB1 expression. FEBS Lett. 507.
Liu, D., Zhang, Z., Kong, C.-z., 2013. High FOXM1 expression was associated with bladder carcinogenesis. Tumour Biol. 34 (2), 1131–1138. http://dx.doi.org/10.1007/s13277-013-0654-x.
Ludwig, T.E., Bergendahl, V., Levenstein, M.E., Yu, J., Probasco, M.D., Thomson, J.A., 2006. Feeder-independent culture of human embryonic stem cells. Nat. Methods 3 (8), 637–646. http://dx.doi.org/10.1038/nmeth902.
Maynard, S., Swistowska, A.M., Lee, J.W., Liu, Y., Liu, S.T., Da Cruz, A.B., ... Bohr, V.A., 2008. Human embryonic stem cells have enhanced repair of multiple forms of DNA damage. Stem Cells 26 (9), 2266–2274. http://dx.doi.org/10.1634/stemcells.2007-1041.
Myatt, S.S., Lam, E.W., 2007. The emerging roles of forkhead box (Fox) proteins in cancer. Nat. Rev. Cancer 7 (11), 847–859. http://dx.doi.org/10.1038/nrc2223.
Neganova, I., Tilgner, K., Buskin, A., Paraskevopoulou, I., Atkinson, S.P., Peberdy, D., ... Lako, M., 2014. CDK1 plays an important role in the maintenance of pluripotency and genomic stability in human pluripotent stem cells. Cell Death Dis. 5, e1508. http://dx.doi.org/10.1038/cddis.2014.464.
Nichols, J., Smith, A., 2009. Naive and primed pluripotent states. Cell Stem Cell 4 (6), 487–492. http://dx.doi.org/10.1016/j.stem.2009.05.015.
Park, H.J., Carr, J.R., Wang, Z., Nogueira, V., Hay, N., Tyner, A.L., ... Raychaudhuri, P., 2009. FoxM1, a critical regulator of oxidative stress during oncogenesis. EMBO J. 28 (19), 2908–2918. http://dx.doi.org/10.1038/emboj.2009.239.
Pekkanen-Mattila, M., Pelto-Huikko, M., Kujala, V., Suuronen, R., Skottman, H., Aalto-Setälä, K., Kerkelä, E., 2010. Spatial and temporal expression pattern of germ layer markers during human embryonic stem cell differentiation in embryoid bodies. Histochem. Cell Biol. 133 (5), 595–606. http://dx.doi.org/10.1007/s00418-010-0689-7.
Pera, M.F., Tam, P.P., 2010. Extrinsic regulation of pluripotent stem cells. Nature 465 (7299), 713–720. http://dx.doi.org/10.1038/nature09228.
Quinlan, A.R., Hall, I.M., 2010. BEDTools: a flexible suite of utilities for comparing genomic features. Bioinformatics 26 (6), 841–842. http://dx.doi.org/10.1093/bioinformatics/btq033.
Ruiz, S., Panopoulos, A.D., Herrerias, A., Bissig, K.D., Lutz, M., Berggren, W.T., ... Izpisua Belmonte, J.C., 2011. A high proliferation rate is required for cell reprogramming and maintenance of human embryonic stem cell identity. Curr. Biol. 21 (1), 45–52. http://dx.doi.org/10.1016/j.cub.2010.11.049.
Sanders, D.A., Gormally, M.V., Marsico, G., Beraldi, D., Tannahill, D., Balasubramanian, S., 2015. FOXM1 binds directly to non-consensus sequences in the human genome. Genome Biol. 16 (1), 130. http://dx.doi.org/10.1186/s13059-015-0696-z.
Sperger, J.M., Chen, X., Draper, J.S., Antosiewicz, J.E., Chon, C.H., Jones, S.B., ... Thomson, J.A., 2003. Gene expression patterns in human embryonic stem cells and human pluripotent germ cell tumors. Proc. Natl. Acad. Sci. U. S. A. 100 (23), 13350–13355. http://dx.doi.org/10.1073/pnas.2235735100.
Tan, G., Cheng, L., Chen, T., Yu, L., Tan, Y., 2014. Foxm1 mediates LIF/Stat3-dependent self-renewal in mouse embryonic stem cells and is essential for the generation of induced pluripotent stem cells. PLoS One 9 (4), e92304. http://dx.doi.org/10.1371/journal.pone.0092304.
Thomson, J.A., Itskovitz-Eldor, J., Shapiro, S.S., Waknitz, M.A., Swiergiel, J.J., Marshall, V.S., Jones, J.M., 1998. Embryonic Stem Cell Lines Derived from Human Blastocysts. Science 282 (5391), 1145–1147. http://dx.doi.org/10.1126/science.282.5391.1145.
Trounson, A., 2006. The production and directed differentiation of human embryonic stem cells. Endocr. Rev. 27 (2), 208–219. http://dx.doi.org/10.1210/er.2005-0016.
Valbuena, D., Galan, A., Sanchez, E., Poo, M.E., Gomez, E., Sanchez-Luengo, S., ... Simon, C., 2006. Derivation and characterization of three new Spanish human embryonic stem cell lines (VAL -3 -4 -5) on human feeder and in serum-free conditions. Reprod. BioMed. Online 13 (6), 875–886.
Wang, X., Kiyokawa, H., Dennewitz, M.B., Costa, R.H., 2002. The Forkhead Box m1b transcription factor is essential for hepatocyte DNA replication and mitosis during mouse liver regeneration. Proc. Natl. Acad. Sci. U. S. A. 99 (26), 16881–16886. http://dx.doi.org/10.1073/pnas.252570299.
Wang, I.C., Chen, Y.J., Hughes, D., Petrovic, V., Major, M.L., Park, H.J., ... Costa, R.H., 2005. Forkhead box M1 regulates the transcriptional network of genes essential for mitotic progression and genes encoding the SCF (Skp2-Cks1) ubiquitin ligase. Mol. Cell. Biol. 25 (24), 10875–10894. http://dx.doi.org/10.1128/MCB.25.24.10875-10894.2005.
Wierstra, I., 2013a. FOXM1 (Forkhead box M1) in tumorigenesis: overexpression in human cancer, implication in tumorigenesis, oncogenic functions, tumor-suppressive properties, and target of anticancer therapy. Adv. Cancer Res. 119, 191–419. http://dx.doi.org/10.1016/b978-0-12-407190-2.00016-2.
Wierstra, I., 2013b. The Transcription Factor FOXM1 (Forkhead box M1): Proliferation-Specific Expression, Transcription Factor Function, Target Genes, Mouse Models, and Normal Biological Roles (2013/06/19 ed. Vol. 118).
Wiseman, E.F., Chen, X., Han, N., Webber, A., Ji, Z., Sharrocks, A.D., Ang, Y.S., 2015. Deregulation of the FOXM1 target gene network and its coregulatory partners in oesophageal adenocarcinoma. Mol. Cancer 14, 69. http://dx.doi.org/10.1186/s12943-015-0339-8.
Wonsey, D.R., Follettie, M.T., 2005. Loss of the forkhead transcription factor FoxM1 causes centrosome amplification and mitotic catastrophe. Cancer Res. 65 (12), 5181–5189.
Xie, Z., Tan, G., Ding, M., Dong, D., Chen, T., Meng, X., ... Tan, Y., 2010. Foxm1 transcription factor is required for maintenance of pluripotency of P19 embryonal carcinoma cells. Nucleic Acids Res. 38 (22), 8027–8038. http://dx.doi.org/10.1093/nar/gkq715.
Young, R.A., 2011. Control of the embryonic stem cell state. Cell 144 (6), 940–954. http://dx.doi.org/10.1016/j.cell.2011.01.032.
Zhang, Y., Liu, T., Meyer, C.A., Eeckhoute, J., Johnson, D.S., Bernstein, B.E., ... Liu, X.S., 2008. Model-based analysis of ChIP-Seq (MACS). Genome Biol. 9 (9), R137. http://dx.doi.org/10.1186/gb-2008-9-9-r137.
Zhang, X., Yalcin, S., Lee, D.F., Yeh, T.Y., Lee, S.M., Su, J., ... Ghaffari, S., 2011. FOXO1 is an essential regulator of pluripotency in human embryonic stem cells. Nat. Cell Biol. 13 (9), 1092–1099. http://dx.doi.org/10.1038/ncb2293.